iScience

CellPress
OPEN ACCESS

Article

Type III adenylyl cyclase is essential for follicular development in female mice and their reproductive lifespan

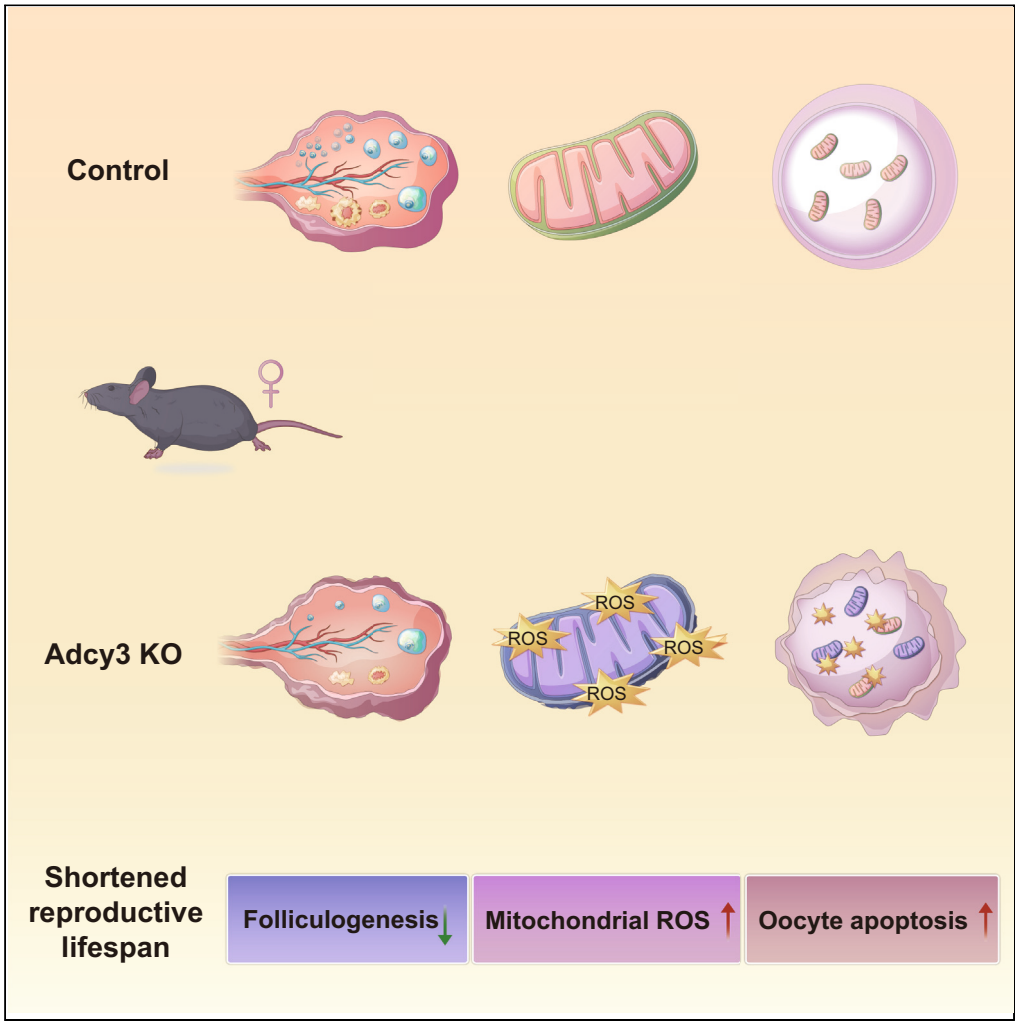

Baofang Zheng, Xiaoyu Hu, Yuanhui Hu, ..., Yongdi Wang, Weina Wang, Zhenshan Wang

xiaoyu.hu@hbu.edu.cn (X.H.)
zswang@hbu.edu.cn (Z.W.)

Highlights

Female mice lacking Adcy3 display a shortened reproductive lifespan

Adcy3 is indispensable for ovarian follicular development

Loss of Adcy3 enhances mitochondrial oxidative stress and oocyte apoptosis

Zheng et al., iScience 27, 110293
July 19, 2024
https://doi.org/10.1016/j.isci.2024.110293

iScience

CellPress
OPEN ACCESS

Article

Type III adenylyl cyclase is essential for follicular development in female mice and their reproductive lifespan

Baofang Zheng,[1,3] Xiaoyu Hu,[1,2,3,*] Yuanhui Hu,[1] Sheng Dong,[1] Xin Xiao,[1] Haoming Qi,[1] Yongdi Wang,[1] Weina Wang,[1] and Zhenshan Wang[1,2,4,*]

SUMMARY

Premature ovarian failure (POF) is a complex and heterogeneous disease that causes infertility and subfertility. However, the molecular mechanism of POF has not been fully elucidated. Here, we show that the loss of adenylyl cyclase III (Adcy3) in female mice leads to POF and a shortened reproductive lifespan. We found that Adcy3 is abundantly expressed in mouse oocytes. Adcy3 knockout mice exhibited the excessive activation of primordial follicles, progressive follicle loss, follicular atresia, and ultimately POF. Mechanistically, we found that mitochondrial oxidative stress in oocytes significantly increased with age in Adcy3-deficient mice and was accompanied by oocyte apoptosis and defective folliculogenesis. In contrast, compared with wild-type female mice, humanized ADCY3 knock-in female mice exhibited improved fertility with age. Collectively, these results reveal that the previously unrecognized Adcy3 signaling pathway is tightly linked to female ovarian aging, providing potential pharmaceutical targets for preventing and treating POF.

INTRODUCTION

Premature ovarian failure (POF) is a primary cause of fertility deterioration and infertility, affecting 1–3% of women younger than 40 worldwide. POF is a complex and heterogeneous disease characterized by fewer follicles and diminished oocyte quantity and quality.[1] Current treatments for POF include hormone replacement therapy and, more recently, stem cell therapy and mitochondrial activation.[2] However, FDA-approved treatments for POF are still lacking. Therefore, understanding the mechanisms of POF is crucial for improving ovarian quality and extending the female reproductive lifespan with age.

Mammalian ovaries consist of oocytes and somatic cells, including granulosa cells (GCs) and cumulus cells (CCs). Each oocyte is surrounded by GCs and CCs, forming a relatively independent structure called a follicle, which serves as the basic functional unit of the female reproductive system.[3] Two forms of follicles exist in the ovary: dormant primordial follicles and developing follicles.[4] The primordial follicle pool, established during the fetal stage, determines the length of the female reproductive lifespan, and a reduction in primordial follicle pool indicates a shortened reproductive life.[5] Furthermore, activated primordial follicles develop into primary follicles, secondary follicles, preantral follicles, and antral follicles.[6] However, the majority of primordial follicles are eliminated by a process called atresia, and only the dominant follicle can release an egg in mono-ovulating mammals.[7] Clinically, the number of antral follicles on ultrasound in the ovaries correlates with the ovarian reserve. Women with very few antral follicles may be diagnosed with POF.[8] The oocyte in the follicle resumes development in response to gonadotropin stimulation, after which its nuclei–germinal vesicle (GV) is broken. This process lasts until the oocyte reaches metaphase II (MII), after which the oocyte is ready for fertilization and completes nuclear maturation.[9] Therefore, the great number of oocytes at the MII stage is a reliable indicator for high-quality embryos. The defined mechanisms underlying the ovarian aging and oocyte dysfunction are not fully understood.

Nine transmembrane adenylyl cyclases (Adcys) (Adcy1-9) and one soluble Adcy,[10,11] which are essential components of G protein-coupled receptor (GPCR) signaling and catalyze the conversion of adenosine triphosphate (ATP) into cyclic adenosine monophosphate (cAMP), have been identified in mammals. Adcy3 expression has been detected in the reproductive systems of male and female mice.[12,13] Without Adcy3, male mice are infertile.[14] In addition, Adcy3-cAMP signaling is dominant in the neonatal mouse ovary,[15] and cAMP has been implicated in the meiotic arrest of oocytes in both rodents and humans.[12,16] Female mice lacking Adcy3 exhibit defective meiotic arrest and accelerated oocyte maturation.[12] Given the coexistence of multiple Adcy isoforms in oocytes and the complementarity among them, whether Adcy3 plays a role in female ovarian aging and the molecular mechanisms by which Adcy3 regulates ovarian function remain largely unexplored.

[1]School of Life Sciences, Institute of Life Science, Hebei University, Baoding 071002, China
[2]Hebei Basic Science Center for Biotic Interaction, Hebei University, Baoding 071002, China
[3]These authors contributed equally
[4]Lead contact
*Correspondence: xiaoyu.hu@hbu.edu.cn (X.H.), zswang@hbu.edu.cn (Z.W.)
https://doi.org/10.1016/j.isci.2024.110293

In the present study, we confirmed that Adcy3 is the most abundantly expressed isoform in mouse oocytes beginning at puberty. Importantly, we found that Adcy3-deficient mice exhibit accelerated reproductive aging and impaired fertility, resembling human POF. Mechanistically, the loss of Adcy3 increases mitochondrial oxidative stress in oocytes and enhances oocyte apoptosis, ultimately resulting in increased follicular atresia. These findings highlight the mechanism by which Adcy3 signaling is involved in follicular development and ovarian aging, providing a potential drug target for the development of therapeutic strategies to alleviate POF and female infertility.

RESULTS

Adenylyl cyclase III -deficient female mice exhibit a shortened reproductive lifespan

To investigate the role of Adcys in female reproduction, we analyzed the transcript levels of Adcys in the ovaries and oocytes of mice at puberty, specifically at the GV stage on postnatal day 30 (PD30), when the ovaries are rapidly growing. Reverse transcription–polymerase chain reaction (RT–PCR) and qPCR revealed that Adcy3 was the most highly expressed Adcy isoform in the ovaries of pubertal mice (Figure 1A and Figure S1A). Moreover, immunofluorescence analysis (IFA) revealed that Adcy3 was primarily localized to the plasma membranes of oocytes, with a plaque-like distribution at the GV stage (Figure 1B). Similarly, qPCR revealed that Adcy3 was significantly more abundant than other Adcy isoforms in the oocytes at puberty (Figure 1C).

To evaluate whether Adcy3 is essential for female fertility, we obtained *Adcy3* knockout (KO) female mice by crossing *Adcy3*$^{+/-}$ mice as previously described.[17] We confirmed that Adcy3 was completely absent from the ovaries, GCs, and oocytes of the KO mice by western blot and IFA analysis (Figures 1D and 1E and Figure S1B). To investigate the fertility of the KO females, control and Adcy3 KO female mice were mated with fertile adult males at PD60. The fertility test showed that the average litter size of the first generation of KO females did not differ from that of the control group (Figure 1F). However, the average litter size significantly decreased after the first litter, with an average of 7.54 $\pm$ 0.78 (control) versus 2.39 $\pm$ 1.39 (Adcy3 KO) in the second litter and 8.08 $\pm$ 1.04 (control) versus 0.69 $\pm$ 0.85 (Adcy3 KO) in the third litter (Figure 1F). In addition, the total number of pups born to Adcy3 KO females was less than 25% of that born to control females (43.46 $\pm$ 2.11 vs 8.46 $\pm$ 2.85) (Figure 1G). No significant differences in body weight were detected between control and KO newborns (Figure 1H). Furthermore, the KO females became completely infertile after three births (Figure 1F). Taken together, these data indicate that the loss of Adcy3 severely shortens the female reproductive lifespan, with an accelerated decline in fertility associated with aging.

Adenylyl cyclase III is indispensable for ovarian follicular development

To investigate the age-dependent role of Adcy3 in ovarian development, we calculated the gonadal indices of control and KO females using the following formula: gonadosomatic index (GSI) = (gonad weight/total body weight) × 100. Morphological and anatomical observations indicated that the volumes and weights of the ovaries from the KO females were notably reduced at PD30 (Figure S2A-S2D). However, the GSIs of the KO females were significantly greater than those of the control females at PD30 and reached the same levels as the controls at PD60 (Figure 2A). These results suggest that Adcy3 KO females experience accelerated ovarian development during puberty.

Next, to examine the ovarian activity in control and Adcy3 KO female mice, we monitored estrus cyclicity for 21 days using vaginal smears. In female mice, the estrus cycle is divided into four stages, namely, proestrus, estrus, metestrus, and diestrus, which repeat every four to five days.[18] The estrus cycle is a valuable indicator of female reproductive status.[18,19] Notably, the proestrus and estrus stages directly affect ovarian development and fertility because ovulation occurs during these stages.[20] Here, we observed that the estrus cycle is dysregulated in Adcy3 KO female mice (Figure 2B). Moreover, vaginal smear analysis revealed that the estrus cycle was significantly prolonged in KO females, with shorter estrus and metestrus phases and a much longer diestrus phase (Figures 2B and 2C). Taken together, our data substantiate the importance of Adcy3 in ovarian function.

Subsequently, we examined the ovarian morphology of Adcy3 KO mice at PD90 using hematoxylin and eosin (H&E) staining. H&E staining revealed a greater number of empty and atretic follicles in the ovaries of the KO mice (Figures 2D and 2E), indicating impaired folliculogenesis. Moreover, we quantified the follicles at different stages and observed a significant reduction in the number of primordial follicles, preantral follicles, and antral follicles in the KO mice (Figures 2F-2H). Consistently, only a small portion of primordial follicles successfully developed into antral follicles and formed corpus lutea (CLs) in KO mice (Figure 2I). This explains why Adcy3 KO mice exhibit normal fertility at a young age but experience an accelerated loss of fertility with age. In addition, we performed senescence-associated β-galactosidase (SA-β-gal) staining to assess cellular senescence.[21,22] We observed that the loss of Adcy3 accelerated senescence, as shown by stronger SA-β−gal staining in follicles than in control females at PD90 (Figure S2E). This result indicates that the loss of Adcy3 leads to premature ovarian aging in mice. Taken together, the above results demonstrate that ovarian follicles experience halted development in the absence of Adcy3, leading to the premature depletion of primordial follicle pools and early fertility termination.

Adenylyl cyclase III deletion accelerates the progressive loss of follicles and results in premature ovarian failure in female mice

To determine the mechanisms underlying subfertility, we monitored follicular development in Adcy3 KO females at various ages by analyzing ovarian morphology. Neither the cyst structure nor the germ cell number was altered at PD2 (Figure 3A). However, at PD7, the KO mice possessed fewer primordial follicles, more primary follicles, and an almost equal number of secondary follicles compared to control mice (Figure 3B). At PD30, the number of primordial follicles in the KO mice was half that in the control mice. In addition, there was a significant increase in the number of secondary follicles, preantral follicles, CLs, and atretic follicles, and this change was accompanied by the upregulation of the

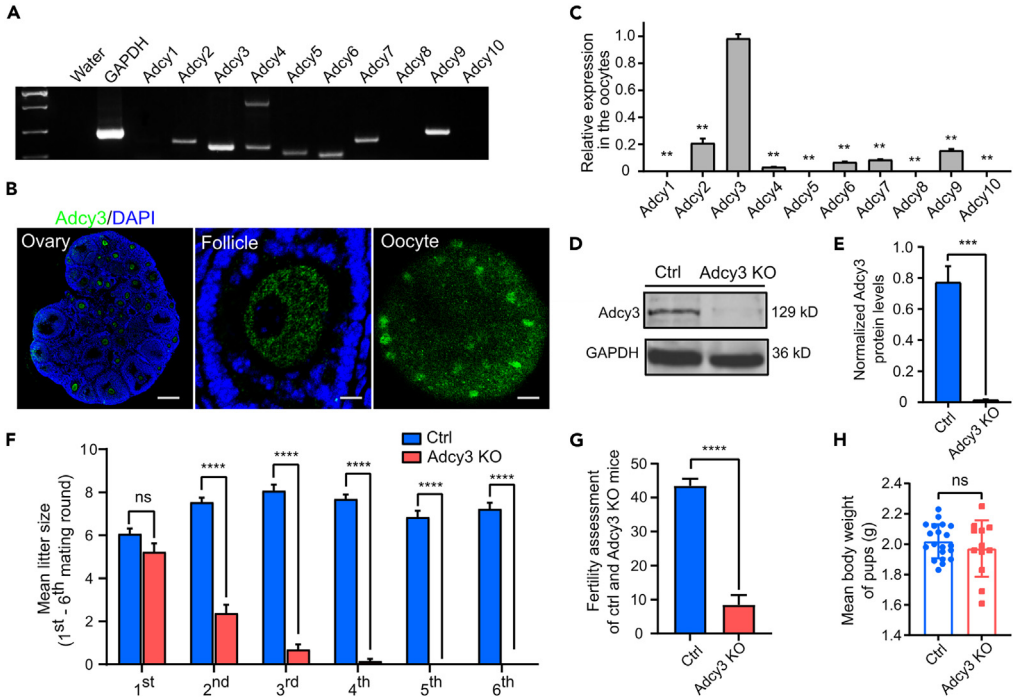

Figure 1. Adcy3 deficient female mice exhibit impaired fecundity

(A) RT-PCR analysis of *Adcy1* to *Adcy10* in the ovaries from female mice at PD30.

(B) Representative images of ovaries and oocytes collected from control females were stained with anti-Adcy3 (green) antibody. DAPI (blue) was used to stain nuclei. Scale bars, 200 μm, 20 μm and 10 μm.

(C) Transcript levels of *Adcy1* to *Adcy10* were quantified by qPCR in the oocytes from female mice at PD30. n = 3 mice per group.

(D and E) Western blot probing with anti-Adcy3 in ovaries from control and Adcy3 KO female mice. GAPDH was used as a loading control. n = 3 mice per group.

(F–H) The average litter size (F), total pups (G), and body weight of pups (H) in control and Adcy3 KO female mice during 6-month breeding trials. n = 13 mice per group. All data were presented as mean ± SD; ns, not significant; $^{**}p < 0.01$, $^{***}p < 0.001$, $^{****}p < 0.0001$ by Student's t-test or one-way ANOVA followed by the Dunnett's multiple comparisons. See also Figure S1.

secretion of the anti-Mullerian hormone (AMH), a reliable indicator of folliculogenesis (Figure 3C and S3A). This finding suggested that the loss of Adcy3 leads to the excessive depletion of the primordial follicle reserve. Furthermore, apparent CL structures were observed in both control and KO mice, suggesting that KO females could ovulate, but the oocytes were prematurely released before the LH peak (Figure 3C). Additionally, only a small number of primordial, primary, and secondary follicles were found, and no developing follicular structures were observed in the ovaries of the KO mice at PD120 (Figure 3D).

Moreover, we quantified the number of primordial follicles in control and KO mice from PD2 to PD120. The number of primordial follicles decreased significantly beginning at PD7 in Adcy3 KO mice, after which the number of primordial follicles rapidly decreased (Figure 3E). Furthermore, we used DDX4, a specific marker of germ cells, to label oocytes and accurately count them. The IFA and western blot results showed that DDX4 expression levels were significantly lower in the KO mice than in the control mice at PD30 and PD120 (Figure S3B-S3I). Taken together, these results indicate that Adcy3 plays a crucial role in preserving follicular development by inhibiting the excessive activation and progressive loss of follicles.

The clinical features of POF are often associated with elevated follicle-stimulating hormone (FSH) and decreased estrogen levels in individuals younger than 40 years.[23,24] Therefore, we measured the serum sex hormone levels in control and Adcy3 KO females at PD90. FSH levels in the KO mice were significantly elevated (Figure 3F). In contrast, the LH and estrogen (E2) levels were significantly decreased in the KO mice (Figures 3G and 3H). However, testosterone levels did not differ between control and KO mice (Figure S3J). Echoing the changes in hormone levels, estrogen receptor (ER) expression was downregulated in the ovaries of Adcy3 KO mice, while the levels of the progesterone receptor (PR) isoforms PR-A and PR-B remained unchanged (Figures 3I and 3J). Furthermore, qPCR and western blot analyses revealed that the expression of inhibin α (INHA), a POF marker,[25] was downregulated in KO mice at PD90 (Figure S3K-S3M). Taken together, our data revealed that the loss of Adcy3 causes defective folliculogenesis in mice, mimicking human female reproductive aging.

Loss of adenylyl cyclase III reduces oocyte quality by inducing oocyte apoptosis

Oocytes play a crucial role in folliculogenesis by directing follicular assembly, and ovarian aging is often accompanied by deteriorations in both the quality and quantity of oocytes. Given that there were more atretic follicles in Adcy3-defective mice (Figure 2E), we administered

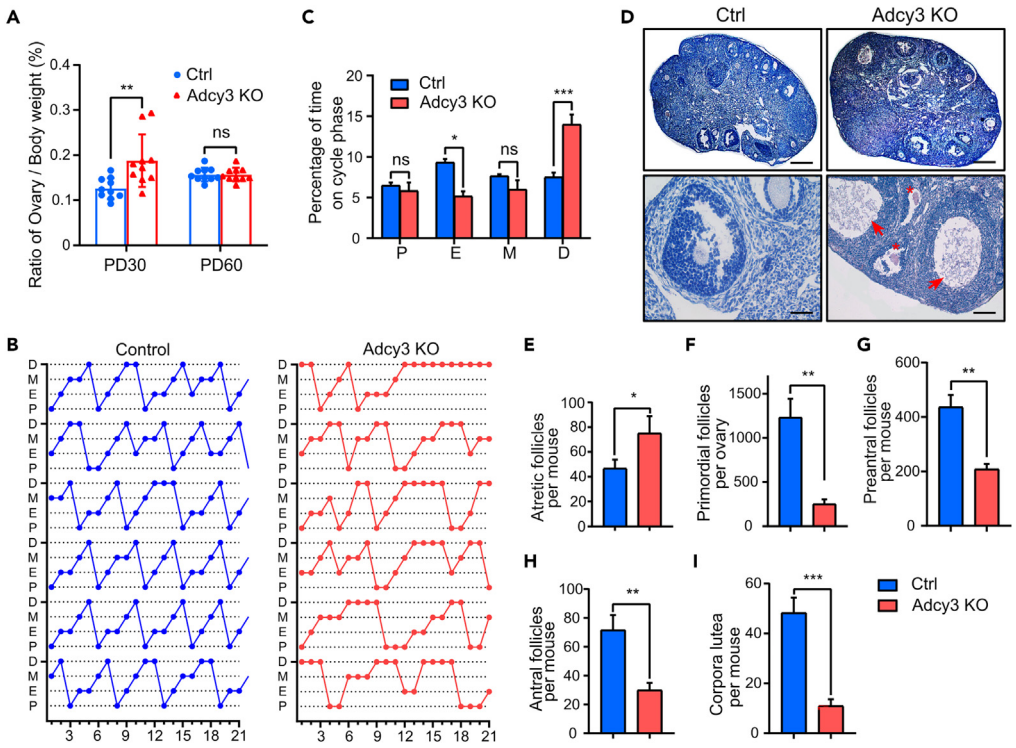

Figure 2. Adcy3 is indispensable for ovarian development and oocyte maturation

(A) The ratio of the ovary to body weight in control and Adcy3 KO female mice at PD30 and PD60. n = 10 mice per group.

(B) Determination of estrous cycles in control and Adcy3 KO female mice at PD90 by hematoxylin and eosin (H&E) staining of mouse vaginal smears. n = 6 mice per group.

(C) Quantification of the length and phases of the estrous cycle in B. P proestrus stage, E estrus stage, M metestrus stage, D diestrus stage. n = 6 mice per group.

(D) Representative images of H&E staining of ovaries from control and Adcy3 KO mice at PD90. Red arrows: empty ovarian follicles; Red asterisk: atretic ovarian follicles. Scale bars, 200 μm (top) and 20 μm (bottom).

(E–I) Quantification of the atretic follicles (E), primordial follicles (F), preantral follicles (G), antral follicles (H), and corpora lutea (I). n = 3 mice per group. All data were presented as mean ± SD; ns, not significant; *$p < 0.05$, **$p < 0.01$, ***$p < 0.001$ by Student's t-test or one-way ANOVA followed by the Dunnett's multiple comparisons. See also Figure S2.

exogenous gonadotropin (PMSG/hCG) to control and Adcy3 KO females and quantified the number of oocytes at the GV and MII stages. At PD30, the oocytes with intact GV membranes were collected and maintained in M2 medium for 16 h. Germinal vesicle breakdown (GVBD) and first polar body extrusion indicate that the oocytes are at meiotic metaphase II.[26] Here, we found that the deletion of Adcy3 increased the occurrence of GVBD (Figure 4A), which promoted the resumption of oocyte meiosis and resulted in early follicular development. At PD90, the number of mature ovulated oocytes released in KO mice was reduced, and the oocytes in the MII stage in KO mice exhibited fragmentation (Figures 4B–4D), indicating that oocyte development was severely impaired in KO mice.

During ovarian development, 99% of germ cells undergo apoptosis and are eliminated through follicular atresia, while the remaining 1% further mature into oocytes. Excessive apoptosis depletes the ovarian reserve, severely impairing folliculogenesis.[27] To address whether Adcy3 signaling regulates ovarian development by modulating apoptosis, we examined cell apoptosis in the ovaries of control and Adcy3 KO mice at PD30 by staining for caspase-3, a key apoptosis mediator. IFA revealed that caspase-3 was predominantly present in the oocytes of the KO mice at PD30 (Figures 4E and 4F), indicating that without Adcy3, the oocytes exhibited early apoptosis even before puberty. We then determined the expression levels of procaspase-3 and cleaved (activated) caspase-3 in the ovaries of control and KO mice. Western blot analysis revealed significantly elevated cleaved caspase-3 expression in the ovaries of the KO mice (Figures 4G and 4H). B-cell lymphoma 2 (Bcl-2) and Bcl-2 associated C protein (Bax) are two apoptotic regulators. Bcl-2 inhibits apoptosis by regulating the release of cytochrome *c* from the mitochondria, whereas Bax oligomerization accelerates cell death by facilitating mitochondrial membrane permeabilization.[28] Western blot analysis revealed that Bcl-2 expression was downregulated, while Bax expression was upregulated (Figure 4I) in the ovaries of KO mice, resulting in a significant reduction in the Bcl-2/Bax ratio (Figure 4J). This result indicated that apoptosis in the ovaries of the KO mice was enhanced. Furthermore, we used a *terminal deoxynucleotidyl transferase dUTP nick end labeling* (TUNEL) assay to detect ovarian apoptosis. We observed that the TUNEL-positive cells were concentrated in the preantral follicles near the oocytes, suggesting that the observed GC apoptosis may be partially due to oocyte apoptosis (Figures 4K and 4L).

In addition, to assess cell proliferation in the ovaries, we determined the protein levels of Ki-67, which is specifically expressed during the active phases of the cell cycle. The IFA results showed that Ki-67-positive GCs were mainly and equally distributed in the secondary follicles

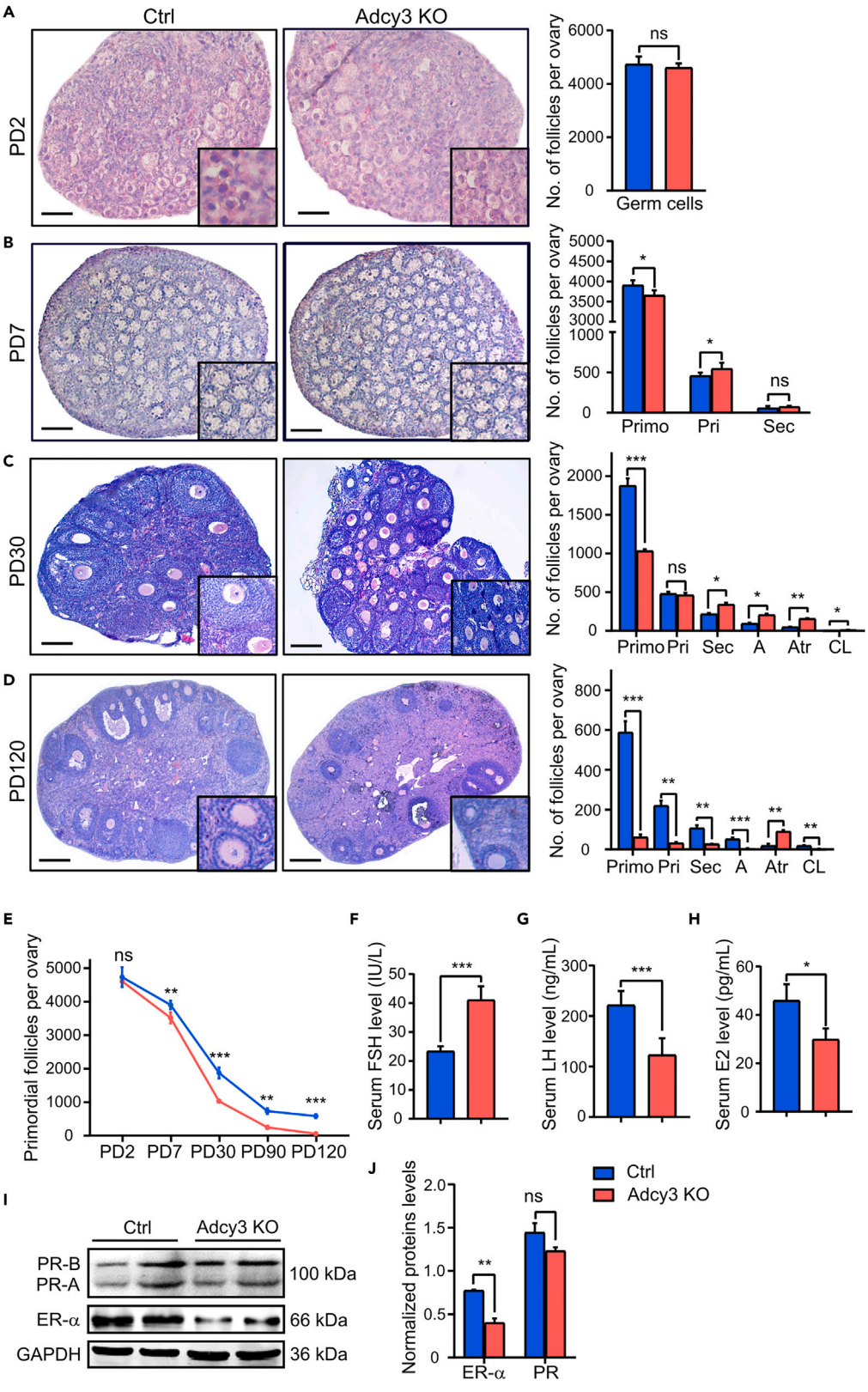
A
Ctrl
Adcy3 KO
PD2
No. of follicles per ovary
ns
Germ cells
B
PD7
Primo
Pri
Sec
C
PD30
Primo Pri Sec A Atr CL
D
PD120
E
Primordial follicles per ovary
PD2 PD7 PD30 PD90 PD120
F
Serum FSH level (IU/L)
G
Serum LH level (ng/mL)
H
Serum E2 level (pg/mL)
I
PR-B
PR-A
100 kDa
ER-α
66 kDa
GAPDH
36 kDa
J
Normalized proteins levels
ER-α
PR

Figure 3. Adcy3 deletion in female mice accelerates the progressive loss of follicles and results in POF

(A–D) Representative images of H&E staining of ovaries from control and Adcy3 KO mice at PD2 (A), PD7 (B), PD30 (C) and PD120 (D), and quantification of follicles in PD2 (A), PD7 (B), PD30 (C) and PD120 (D) female mice. Scale bars, A-B = 50 μm and C-D = 200 μm. Abbreviations: primordial (Primo), primary (Pri), secondary (Sec), antral (A), Atr (Atretic) follicles, and corpora lutea (CL).

(E) Quantification of primordial follicles in control and Adcy3 KO mice from PD2 to PD120.

(F–H) The serum levels of FSH (F), LH (G) and E2 (H) were measured by ELISA from control and Adcy3 KO female mice. n = 3 mice per group.

(I and J) Western blot probing with anti-PR-B, anti-PR-A, and anti-ER-α in ovaries from control and Adcy3 KO female mice. GAPDH was used as a loading control. n = 3 mice per group. All data were presented as mean ± SD; ns, not significant; *$p < 0.05$, **$p < 0.01$, ***$p < 0.001$ by Student's t-test or one-way ANOVA followed by the Dunnett's multiple comparisons. See also Figure S3.

and early antral follicles (Figure S4A and S4B). Similarly, EdU staining revealed no differences in cell proliferation between control and KO female mice (Figure S4C and S4D), indicating that the lack of Adcy3 did not affect GC proliferation. In conclusion, these data demonstrate that the loss of ovarian follicles in Adcy3 KO mice is primarily caused by excessive oocyte apoptosis.

Ablation of adenylyl cyclase III enhances mitochondria-mediated oxidative stress in oocytes

To investigate the mechanisms underlying the shortened reproductive lifespan caused by Adcy3 deficiency, we collected ovaries from control and KO female mice. We then conducted proteomics analysis to identify the differentially expressed proteins (DEPs) in the ovary and the essential components that result in female reproductive aging upon Adcy3 deletion. A total of 284 DEPs, including 122 significantly upregulated proteins and 162 downregulated proteins, were identified in Adcy3 KO mice (Figure 5A and Table S1). Adcy3-cAMP signaling is essential for metabolism-related signal transduction.[29] In line with this function, numerous DEPs revealed by our proteomic analysis were involved in metabolic pathways (Figure S5A). Accordingly, we focused on those DEPs that showed significant enrichment in metabolic pathways. Gene Ontology (GO) enrichment analysis indicated that these DEPs were involved primarily in oxidation–reduction processes and were enriched in mitochondria and exosomes (Figure 5B). Thus, it is reasonable to hypothesize that ovarian aging in Adcy3 KO mice is mainly attributed to mitochondrial dysfunction.

To determine whether Adcy3 ablation leads to mitochondrial dysfunction, we first observed the mitochondrial morphology in oocytes at the GV and MII stages by MitoTracker staining. IFA revealed that the mitochondria were either evenly distributed in the cytoplasm or clustered at the periphery of the GV-stage oocytes in both the control and KO mice (i and ii, Figures 5C and 5D). Similarly, two mitochondrial distribution patterns were observed in oocytes in the MII stage, termed iii and iv (Figure 5C and 5D). However, there were fewer mitochondria, which also exhibited a greater degree of fragmentation, in the MII-stage ovaries in the KO mice compared with those in the control mice (Figures 5C and 5D), resembling the distribution of mitochondria in aged oocytes.[30,31] Reportedly, mitochondria produce the majority of the reactive oxygen species (ROS) in the ovaries during folliculogenesis.[32] Excess cellular ROS causes cell damage, which can lead to apoptosis.[33] Therefore, we assessed the ROS levels in oocytes utilizing the fluorescent probe DCFH-DA. The staining results revealed that the ROS content was increased 6.4-fold in the KO mouse oocytes compared to that in the control oocytes (Figures 5E and 5F). Taken together, our data indicate that the loss of Adcy3 signaling disrupts mitochondrial function in oocytes mainly by enhancing mitochondrial oxidative stress.

Humanized adenylyl cyclase III knock-in mice exhibit ameliorated natural aging-induced premature ovarian failure

We used humanized ADCY3 knock-in mice (hADCY3 mice), which we previously established,[34] to investigate the role of human ADCY3 in female reproduction. First, we examined ADCY3 expression levels in the ovaries of hADCY3 mice. qPCR and western blot showed that Adcy3 levels were greater in the ovaries of hADCY3 mice than in the ovaries of control mice (Figures 6A–6C). Next, control and hADCY3 females were mated with fertile adult males, and the litter sizes were quantified. The results revealed that the natural aging hADCY3 (NA-hADCY3) mice produced more pups in each litter before the 10th litter, although no significant differences were found in the body weights of the pups (Figures 6D and 6E).

Next, we examined folliculogenesis in control and hADCY3 mice by counting follicles in the ovaries. We observed that the germ cells were not altered at PD2 (Figure 6F). However, the primordial and developing follicles were more abundant in the hADCY3 mice than in control mice at PD7 and PD30 (Figures 6G and 6H). Furthermore, we observed more primordial and developing follicles and fewer atretic follicles in the hADCY3 mice at PD60 and PD90 (Figures 6I and 6J). This finding indicates that human ADCY3 delays ovarian aging in female mice by protecting primordial follicles and suppressing follicular atresia.

Similarly, qPCR revealed a significant increase in the expression level of AMH in NA-hADCY3 mice (Figure 6K), which is indicative of ameliorated ovarian function. Reportedly, aged mice release fewer oocytes with an increased percentage of abnormal oocytes upon superovulation.[35] Here, we found that the percentage of ovulated oocytes was significantly greater in NA-hADCY3 mice than in control mice, whereas the percentage of abnormally ovulated oocytes in NA-hADCY3 mice was lower (Figures 6L and 6M), indicating that hADCY3 addition effectively alleviated mouse ovarian senescence and extended the reproductive lifespan of female mice.

DISCUSSION

In this study, we found that Adcy3 is the predominant Adcy isoform in mouse oocytes during puberty and adulthood. Reportedly, Adcy3 is expressed in the cilia of neuronal cells, including olfactory cells, and plays essential roles in olfaction and other physiological processes in mammals.[34,36–38] However, its physiological role in female ovarian function has not been fully elucidated. Here, we demonstrated that

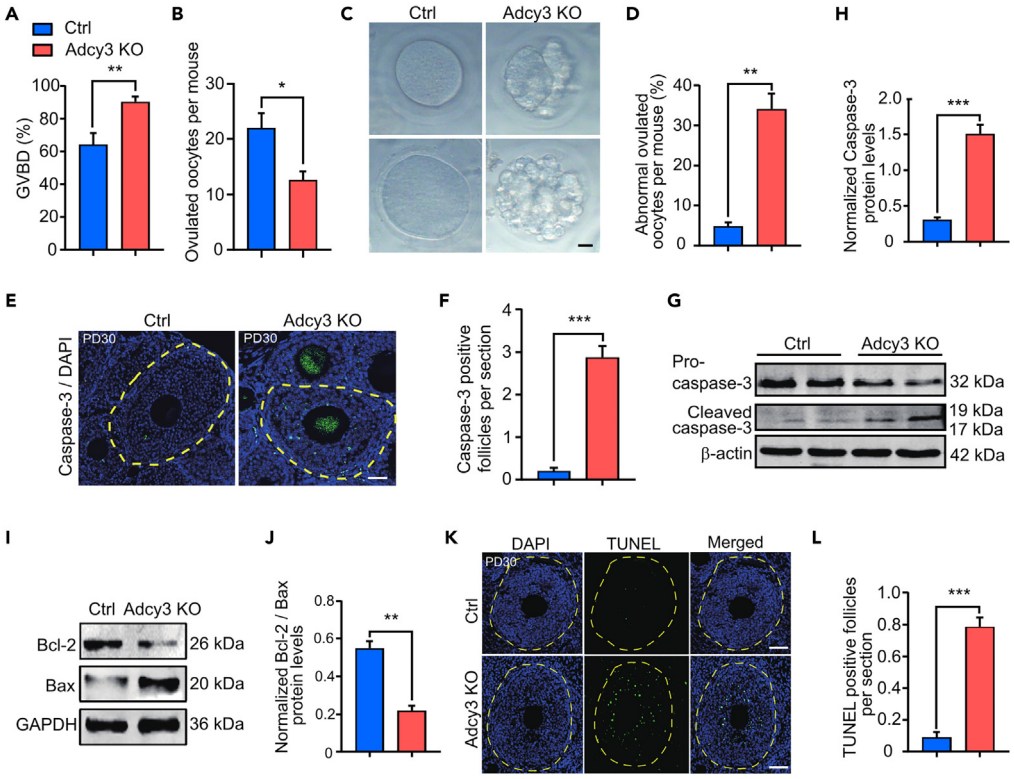

Figure 4. Loss of Adcy3 increases oocyte apoptosis

(A) Percentage of GVBD of oocytes in control and Adcy3 KO female mice.

(B) Quantification of the ovulated oocytes per mouse in control and Adcy3 KO female mice.

(C) Representative images of oocytes at the MII stage collected from control and Adcy3 KO female mice. Scale bar, 20 μm.

(D) Quantification of the abnormal ovulated oocytes per mouse from control and Adcy3 KO female mice.

(E) Ovaries collected from control and Adcy3 KO females were stained with anti-caspase-3 (green) antibody. DAPI (blue) was used to stain nuclei. Scale bar, 20 μm.

(F). Quantitative analysis of caspase-3 positive follicles per section in (E).

(G and H) Western blot probing with anti-procaspase-3 and anti-cleaved caspase-3 of ovaries from control and Adcy3 KO female mice. β-actin was used as a loading control.

(I and J) Western blot probing with anti-BCL2 and anti-BAX of ovaries from control and Adcy3 KO female mice. GAPDH was used as a loading control.

(K) Representative images of follicular apoptosis by TUNEL staining of ovaries from control and Adcy3 KO female mice. Scale bars, 20 μm.

(L) Quantification of TUNEL-positive follicles in ovaries from mice in each group. n = 3 mice per group. All data were presented as mean ± SD; ns, not significant; *$p < 0.05$, **$p < 0.01$, ***$p < 0.001$ by Student's t-test or one-way ANOVA followed by the Dunnett's multiple comparisons. See also Figure S4.

mice lacking Adcy3 exhibited a progressive loss of ovarian follicles and accelerated oocyte aging, a phenotype that is reminiscent of typical human POF. Moreover, we demonstrated that this phenotype is accompanied by mitochondrial dysfunction, exacerbated oxidative stress, and enhanced oocyte apoptosis.

Furthermore, we observed that newborn female mice developed a normal primordial follicle reserve at PD2, which is consistent with the finding that Adcy2 is the predominant isoform in perinatal ovaries.[39] However, the primordial follicle reserve is depleted beginning at puberty when Adcy3 is knocked out. By the time of sexual maturity, the primordial follicle pool was almost exhausted, and the number of developing follicles at all stages decreased significantly. In addition, compared with those in control females, there were significantly more atretic and apoptotic follicles in Adcy3 KO mice, and these changes substantially contributed to ovarian aging and subfertility. Therefore, we conclude that Adcy3 is the primary Adcy isoform in mouse ovaries during puberty and adulthood and that it can cooperate with Adcy2 to regulate normal ovary development in a spatiotemporal manner. Given that the Adcy3 proteins in mice and humans share more than 80% homology, we speculate that human ADCY3 might exert similar regulatory effects on human ovarian development. In this sense, mice represent a reliable model for dissecting the role of ADCY3 in human reproduction.

In our study, we found that the average litter size of the KO females was comparable to that of the control females in the first generation, suggesting that Adcy3 deficiency does not affect fertility in young females (Figure 1F). However, oocyte quality and female fertility in Adcy3-deficient mice decreased and subsequently deteriorated with age. Furthermore, we showed that the absence of Adcy3 leads to POF and oocyte apoptosis, leading us to conclude that Adcy3 plays a major role in maintaining the duration of the reproductive lifespan.

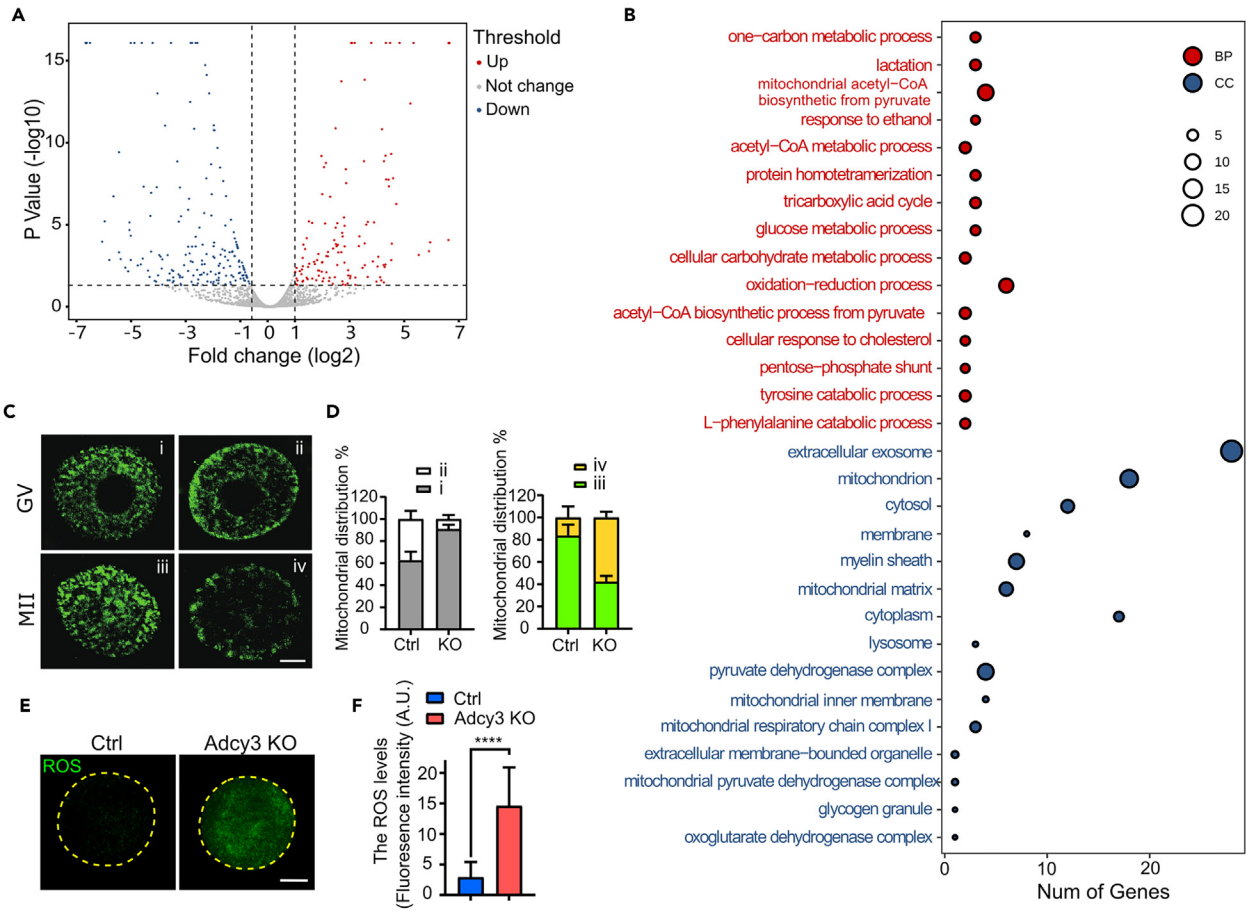

Figure 5. Ablation of Adcy3 enhances mitochondria-mediated oxidative stress in oocytes

(A) Volcano plot of differentially expressed proteins between control and Adcy3 KO mouse ovaries. The upregulated and downregulated proteins (upregulated > two-fold-change or downregulated <0.67-fold-change, $p < 0.05$) were highlighted in red and blue, respectively. Gray spots indicate no differences in protein expression levels.

(B) Gene ontology enrichment analysis of the differentially expressed genes that are enriched in the metabolic pathway in the ovaries of control and Adcy3 KO mice, and was ordered by *p*-value.

(C) Representative images of mitochondrial distribution patterns in oocytes at GV (i and ii) and MII (iii and iv) phases from control and Adcy3 KO female mice. Scale bar, 25 μm.

(D) Quantification of mitochondrial distribution patterns in oocytes at GV (i and ii) and MII (iii and iv) stages from control and Adcy3 KO mice as indicated.

(E) Representative images of ROS levels detected by DCFH-DA staining in oocytes from control and Adcy3 KO females at PD60. Scale bar, 20 μm.

(F) Quantification of the fluorescence intensity of ROS signals was measured in control (n = 10), and Adcy3 KO (n = 10) female oocytes. All data were presented as mean ± SD; ns, not significant; ****$p < 0.0001$ by Student's t-test or one-way ANOVA followed by the Dunnett's multiple comparisons. See also Figure S5 and Table S1.

Mitochondria are dynamic organelles that maintain energy homeostasis and coordinate cellular responses to stress, such as nutrient deficiency and oxidation.[40] Excessive stress can cause mitochondrial dysfunction and eventually cell apoptosis.[40,41] Oocytes contain enriched mitochondria, indicating the importance of the mitochondria in female reproduction.[42] Impaired mitochondrial function leads to oocyte senescence and ovarian aging.[43,44] For example, the deletion of two mitochondrial fusion proteins, Mitofusins 1 and 2, in oocytes results in increased apoptosis and accelerated POF.[31,45] Coenzyme Q10 supplementation can improve mitochondrial activity and ameliorate oocyte quality in aged mice.[46] In addition, mitochondrial dysfunction disrupts ATP production, which causes ROS overproduction in oocytes and thus decreases oocyte quality.[44] Here, our proteomic analysis, coupled with the impaired mitochondrial distribution in oocytes at the MII stage in Adcy3 KO females, indicated that Adcy3 ablation leads to mitochondrial dysfunction. However, further studies are needed to investigate the underlying molecular mechanisms by which Adcy3 regulates oocyte signaling pathways associated with mitochondrial dysfunction.

POF is characterized by a reduced ovarian follicle reserve and insufficient ovarian sex hormones.[47] Here, we elucidated that Adcy3 ablation induces defective ovarian folliculogenesis, which is accompanied by increased FSH levels and decreased E2 levels in the serum, mimicking the symptoms of human POF. Reportedly, the activity of the female reproductive system is regulated by the hypothalamic-pituitary-ovarian (HPO) axis, mainly through hormonal communication.[48] This axis controls reproduction and aging in animals. The hypothalamus stimulates the

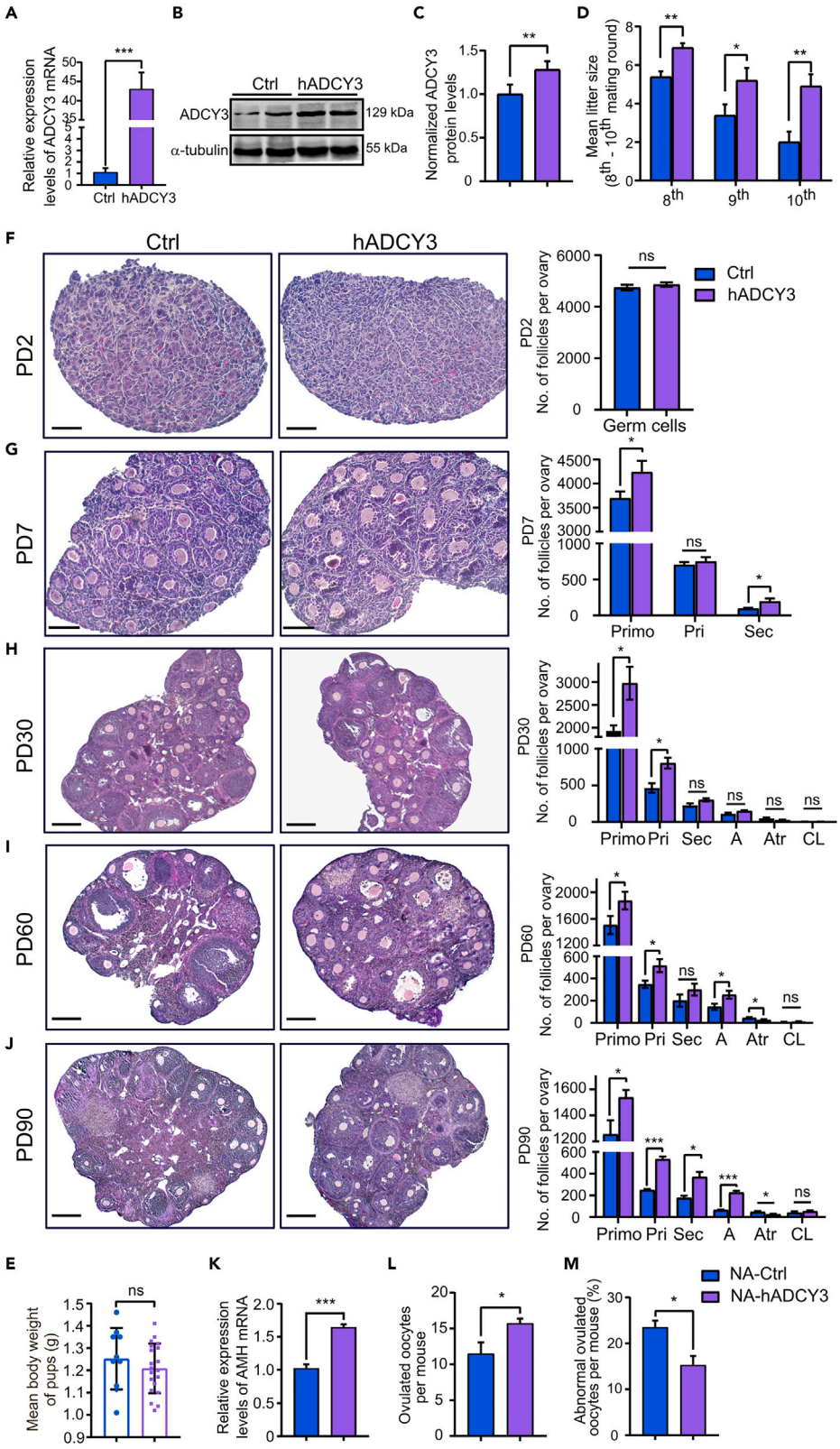
A
Relative expression levels of ADCY3 mRNA
Ctrl
hADCY3
B
Ctrl
hADCY3
ADCY3
129 kDa
α-tubulin
55 kDa
C
Normalized ADCY3 protein levels
D
Mean litter size (8th - 10th mating round)
8th
9th
10th
F
Ctrl
hADCY3
PD2
No. of follicles per ovary
Germ cells
G
PD7
Primo
Pri
Sec
H
PD30
Primo
Pri
Sec
A
Atr
CL
I
PD60
J
PD90
E
Mean body weight of pups (g)
K
Relative expression levels of AMH mRNA
L
Ovulated oocytes per mouse
M
NA-Ctrl
NA-hADCY3
Abnormal ovulated oocytes per mouse (%)

Figure 6. hADCY3 knock-in ameliorates natural aging-induced POF in female mice

(A) Transcript levels of ADCY3 were quantified by qPCR in the ovaries collected from control and hADCY3 female mice.

(B and C) Western blot probing with anti-ADCY3 of ovaries collected from control and hADCY3 female mice. GAPDH was used as a loading control. n = 5 mice per group.

(D and E) The average litter size (D) and body weight of pups (E) in NA-control and NA-hADCY3 female mice of eight-to eleven-month-old.

(F–J) Representative images of H&E staining of ovaries from control and hADCY3 mice at PD2 (F), PD7 (G), PD30 (H), PD60 (I) and PD90 (J), and quantification of follicles in PD2 (F), PD7 (G), PD30 (H), PD60 (I) and PD90 (J) female mice. Scale bars, F-G = 50 μm and H-J = 200 μm. Abbreviations: primordial (Primo), primary (Pri), secondary (Sec), antral (A), Atr (Atretic) follicles, and corpora lutea (CL).

(K) Transcript levels of AMH were quantified by qPCR in the ovaries from NA-control and NA-hADCY3 female mice.

(L) Quantification of the ovulated oocytes per mouse from NA-control and NA-hADCY3 female mice.

(M) Quantification of the abnormal ovulated oocytes per mouse from NA-control and NA-hADCY3 female mice. n = 3 mice per group. All data were presented as mean ± SD; ns, not significant; $*p < 0.05$, $**p < 0.01$, $***p < 0.001$ by Student's t-test or one-way ANOVA followed by the Dunnett's multiple comparisons.

pituitary gland to release FSH and LH, which in turn act on follicles in the ovaries to regulate the synthesis of sex hormones such as estrogens to regulate female fertility.[48,49] During folliculogenesis, FSH and LH act first on the GCs in the outer layer of the follicles by binding to their respective receptors and then extend inward to the oocyte, which plays a dominant role in folliculogenesis.[50] Therefore, GCs are thought to initiate follicular atresia and undergo apoptosis earlier than oocytes in response to hormonal changes.[51] However, our data showed that the majority of Adcy3 is enriched in mouse oocytes but not in GCs during the pubertal and adult stages. Moreover, female mice lacking Adcy3 at PD30 exhibited mainly oocyte apoptosis rather than GC apoptosis. Therefore, we speculate that the shortened reproductive lifespan of Adcy3-deficient mice is primarily caused by deteriorated oocyte quality rather than by the effects of hypothalamic-regulated hormone release on the ovaries.

In oocytes, cAMP signaling regulates oocyte meiotic prophase I, and cAMP levels largely determine meiotic arrest.[52] cAMP is a critical secondary messenger that is synthesized from ATP by Adcys. Targeting the cAMP signaling pathway has been shown to be an effective strategy for treating POF.[53] For instance, an elevated cAMP concentration in the cumulus-oocyte complex enhances intercellular communication and supplies metabolites for oocyte growth.[54] In addition, the cAMP/BDNF pathway has been proposed as a potential therapeutic target for treating POF and infertility.[55,56] In our work, we found that hADCY3 knock-in mice exhibited a longer reproductive lifespan, as evidenced by the significantly increased number of pups per litter. Reportedly, NA control mice often exhibit defective ovarian development and poor oocyte quality.[57] However, we found that the addition of a copy of hADCY3 to the female mouse genome effectively delayed NA-induced POF in mice. The protective role of Adcy3 in female reproduction during aging provides insights into the genetic etiology of POF and potential therapeutic targets.

In summary, we have shown that the depletion of Adcy3 impairs the female reproductive lifespan by inducing oocyte apoptosis. We discovered a previously unrecognized Adcy3 signaling pathway that links mitochondrial dysfunction to oocyte development. We elucidated that Adcy3-deficient females exhibited a high level of follicular atresia and more fragmented oocytes caused by intensified oocyte apoptosis and hence the premature aging of ovarian follicles. Additionally, we found that hADCY3 female mice exhibited an increased reproductive lifespan compared with control mice as they aged. Our findings indicate that Adcy3 deletion accelerates ovarian aging, disrupts mitochondrial function, enhances oxidative stress, and expedites oocyte apoptosis. Thus, our work proposes that maintaining physiological levels of Adcy3 in oocytes is a potential strategy for POF prevention.

LIMITATIONS OF STUDY

There are a few limitations to the current work. One limitation is that, although we demonstrated that Adcy3 is abundantly expressed in mouse oocytes but not GCs, and the effects of hypothalamic-regulated hormone release on ovaries should not be the primary cause of the shortened reproductive life. However, these data could not rule out the possibility that the hypothalamus regulates the reproductive lifespan of the mice lacking Adcy3. Further studies will focus on examining the reproductive lifespan of female mice with the oocyte-specific deletion of Adcy3. Another limitation of our study is that we have not identified the cause of oocyte mitochondrial dysfunction and apoptosis. Further investigations are needed to unravel these mechanisms.

STAR★METHODS

Detailed methods are provided in the online version of this paper and include the following:

- KEY RESOURCES TABLE
- RESOURCE AVAILABILITY
  - Lead contact
  - Materials availability
  - Data and code availability
- EXPERIMENTAL MODEL AND STUDY PARTICIPANT DETAILS
  - Animals
- METHOD DETAILS
  - Fertility assay

SUPPLEMENTAL INFORMATION

Supplemental information can be found online at https://doi.org/10.1016/j.isci.2024.110293.

ACKNOWLEDGMENTS

We thank Hebei University Microscopy Core Facilities for technical assistance with the imaging. This work was supported by the National Natural Science Foundation of China to Z.W. (32070567) and X.H. (32202840); the Natural Science Foundation of Hebei Province of China to X.H. (C2023201032 and C20230308).

AUTHOR CONTRIBUTIONS

B.Z. and X.H. contributed equally to this work. Conceptualization: B.Z., X.H. and Z.W. Investigation, visualization, and analysis: B.Z., X.H., Y.H., S.D., X.X., H.Q., Y.W., W.W., and Z.W. Writing, review, and editing: B.Z., X.H., and Z.W. Supervision: X.H. and Z.W. Project administration and funding acquisition: X.H. and Z.W. All authors read and approved the final version of the revised article.

DECLARATION OF INTERESTS

The authors declare no competing interests.

Received: January 12, 2024
Revised: May 15, 2024
Accepted: June 14, 2024
Published: June 17, 2024

REFERENCES

1. Amargant, F., Manuel, S.L., Tu, Q., Parkes, W.S., Rivas, F., Zhou, L.T., Rowley, J.E., Villanueva, C.E., Hornick, J.E., Shekhawat, G.S., et al. (2020). Ovarian stiffness increases with age in the mammalian ovary and depends on collagen and hyaluronan matrices. Aging Cell *19*, e13259. https://doi.org/10.1111/acel.13259.
2. Huang, Q.Y., Chen, S.R., Chen, J.M., Shi, Q.Y., and Lin, S. (2022). Therapeutic options for premature ovarian insufficiency: an updated review. Reprod. Biol. Endocrinol. *20*, 28. https://doi.org/10.1186/s12958-022-00892-8.
3. Li, H., and Chian, R.-C. (2017). Follicular Development and Oocyte Growth. In Development of In Vitro Maturation for Human Oocytes: Natural and Mild Approaches to Clinical Infertility Treatment, R.-C. Chian, G. Nargund, and J.Y.J. Huang, eds. (Springer International Publishing), pp. 37–57. https://doi.org/10.1007/978-3-319-53454-1_2.
4. Zheng, W., Zhang, H., Gorre, N., Risal, S., Shen, Y., and Liu, K. (2014). Two classes of ovarian primordial follicles exhibit distinct developmental dynamics and physiological functions. Hum. Mol. Genet. *23*, 920–928. https://doi.org/10.1093/hmg/ddt486.
5. Reddy, P., Zheng, W., and Liu, K. (2010). Mechanisms maintaining the dormancy and survival of mammalian primordial follicles. Trends Endocrinol. Metab. *21*, 96–103. https://doi.org/10.1016/j.tem.2009.10.001.
6. ESHRE Capri Workshop Group. Mono-ovulatory cycles: a key goal in profertility programmes. Hum Reprod Update 2003; 9: 263-74. https://doi.org/10.1093/humupd/dmg020.
7. Orisaka, M., Miyazaki, Y., Shirafuji, A., Tamamura, C., Tsuyoshi, H., Tsang, B.K., and Yoshida, Y. (2021). The role of pituitary gonadotropins and intraovarian regulators in follicle development: A mini-review. Reprod. Med. Biol. *20*, 169–175. https://doi.org/10.1002/rmb2.12371.
8. Coelho Neto, M.A., Ludwin, A., Borrell, A., Benacerraf, B., Dewailly, D., da Silva Costa, F., Condous, G., Alcazar, J.L., Jokubkiene, L., Guerriero, S., et al. (2018). Counting ovarian antral follicles by ultrasound: a practical guide. Ultrasound Obstet. Gynecol. *51*, 10–20. https://doi.org/10.1002/uog.18945.
9. Trounson, A., Anderiesz, C., and Jones, G. (2001). Maturation of human oocytes in vitro and their developmental competence. Reproduction *121*, 51–75. https://doi.org/10.1530/rep.0.1210051.
10. Sadana, R., and Dessauer, C.W. (2009). Physiological Roles for G Protein-Regulated Adenylyl Cyclase Isoforms: Insights from Knockout and Overexpression Studies. Neurosignals *17*, 5–22. https://doi.org/10.1159/000166277.
11. Ostrom, K.F., LaVigne, J.E., Brust, T.F., Seifert, R., Dessauer, C.W., Watts, V.J., and Ostrom, R.S. (2022). Physiological roles of mammalian transmembrane adenylyl cyclase isoforms. Physiol. Rev. *102*, 815–857. https://doi.org/10.1152/physrev.00013.2021.
12. Horner, K., Livera, G., Hinckley, M., Trinh, K., Storm, D., and Conti, M. (2003). Rodent oocytes express an active adenylyl cyclase required for meiotic arrest. Dev. Biol. *258*, 385–396. https://doi.org/10.1016/s0012-1606(03)00134-9.

13. Livera, G., Xie, F., Garcia, M.A., Jaiswal, B., Chen, J., Law, E., Storm, D.R., and Conti, M. (2005). Inactivation of the Mouse Adenylyl Cyclase 3 Gene Disrupts Male Fertility and Spermatozoon Function. Mol. Endocrinol. *19*, 1277–1290. https://doi.org/10.1210/me.2004-0318.
14. Chen, T., Zhou, Y., Liu, X., Liu, Y., Yuan, J., and Wang, Z. (2022). Adenylyl cyclase 3 deficiency results in dysfunction of blood-testis barrier during mouse spermiogenesis. Theriogenology *180*, 40–52. https://doi.org/10.1016/j.theriogenology.2021.12.017.
15. Zheng, W., Zhang, T., Zhao, T., Zhu, Z., Qin, S., Yan, H., He, M., Zhou, B., Xia, G., Zhang, H., and Wang, C. (2023). cAMP controls the balance between dormancy and activation of primordial follicles in mouse ovaries. PNAS Nexus *2*, pgad055. https://doi.org/10.1093/pnasnexus/pgad055.
16. DiLuigi, A., Weitzman, V.N., Pace, M.C., Siano, L.J., Maier, D., and Mehlmann, L.M. (2008). Meiotic arrest in human oocytes is maintained by a Gs signaling pathway. Biol. Reprod. *78*, 667–672. https://doi.org/10.1095/biolreprod.107.066019.
17. Wong, S.T., Trinh, K., Hacker, B., Chan, G.C., Lowe, G., Gaggar, A., Xia, Z., Gold, G.H., and Storm, D.R. (2000). Disruption of the type III adenylyl cyclase gene leads to peripheral and behavioral anosmia in transgenic mice. Neuron *27*, 487–497. https://doi.org/10.1016/s0896-6273(00)00060-x.
18. Byers, S.L., Wiles, M.V., Dunn, S.L., and Taft, R.A. (2012). Mouse Estrous Cycle Identification Tool and Images. PLoS One *7*, e35538. https://doi.org/10.1371/journal.pone.0035538.
19. Ajayi, A.F., and Akhigbe, R.E. (2020). Staging of the estrous cycle and induction of estrus in experimental rodents: an update. Fertil. Res. Pract. *6*, 5. https://doi.org/10.1186/s40738-020-00074-3.
20. Lenert, M.E., Chaparro, M.M., and Burton, M.D. (2021). Homeostatic Regulation of Estrus Cycle of Young Female Mice on Western Diet. J. Endocr. Soc. *5*, bvab010. https://doi.org/10.1210/jendso/bvab010.
21. Hall, B.M., Balan, V., Gleiberman, A.S., Strom, E., Krasnov, P., Virtuoso, L.P., Rydkina, E., Vujcic, S., Balan, K., Gitlin, I., et al. (2016). Aging of mice is associated with p16(Ink4a)- and β-galactosidase-positive macrophage accumulation that can be induced in young mice by senescent cells. Aging (Albany NY) *8*, 1294–1315. https://doi.org/10.18632/aging.100991.
22. Debacq-Chainiaux, F., Erusalimsky, J.D., Campisi, J., and Toussaint, O. (2009). Protocols to detect senescence-associated beta-galactosidase (SA-betagal) activity, a biomarker of senescent cells in culture and in vivo. Nat. Protoc. *4*, 1798–1806. https://doi.org/10.1038/nprot.2009.191.
23. Jiao, X., Meng, T., Zhai, Y., Zhao, L., Luo, W., Liu, P., and Qin, Y. (2021). Ovarian Reserve Markers in Premature Ovarian Insufficiency: Within Different Clinical Stages and Different Etiologies. Front. Endocrinol. *12*, 601752.
24. European Society for Human Reproduction and Embryology ESHRE Guideline Group on POI, Webber, L., Davies, M., Anderson, R., Bartlett, J., Braat, D., Cartwright, B., Cifkova, R., de Muinck Keizer-Schrama, S., Hogervorst, E., et al. (2016). ESHRE Guideline: management of women with premature ovarian insufficiency. Hum. Reprod. *31*, 926–937. https://doi.org/10.1093/humrep/dew027.
25. Harris, S.E., Chand, A.L., Winship, I.M., Gersak, K., Nishi, Y., Yanase, T., Nawata, H., and Shelling, A.N. (2005). INHA promoter polymorphisms are associated with premature ovarian failure. Mol. Hum. Reprod. *11*, 779–784. https://doi.org/10.1093/molehr/gah219.
26. Miao, Y.-L., Kikuchi, K., Sun, Q.-Y., and Schatten, H. (2009). Oocyte aging: cellular and molecular changes, developmental potential and reversal possibility. Hum. Reprod. Update *15*, 573–585. https://doi.org/10.1093/humupd/dmp014.
27. Tiwari, M., Prasad, S., Tripathi, A., Pandey, A.N., Ali, I., Singh, A.K., Shrivastav, T.G., and Chaube, S.K. (2015). Apoptosis in mammalian oocytes: a review. Apoptosis *20*, 1019–1025. https://doi.org/10.1007/s10495-015-1136-y.
28. Dlugosz, P.J., Billen, L.P., Annis, M.G., Zhu, W., Zhang, Z., Lin, J., Leber, B., and Andrews, D.W. (2006). Bcl-2 changes conformation to inhibit Bax oligomerization. EMBO J. *25*, 2287–2296. https://doi.org/10.1038/sj.emboj.7601126.
29. Acin-Perez, R., Salazar, E., Kamenetsky, M., Buck, J., Levin, L.R., and Manfredi, G. (2009). Cyclic AMP produced inside mitochondria regulates oxidative phosphorylation. Cell Metab. *9*, 265–276. https://doi.org/10.1016/j.cmet.2009.01.012.
30. Yang, Q., Li, H., Wang, H., Chen, W., Zeng, X., Luo, X., Xu, J., and Sun, Y. (2023). Deletion of enzymes for de novo NAD+ biosynthesis accelerated ovarian aging. Aging Cell *22*, e13904. https://doi.org/10.1111/acel.13904.
31. Chen, W., Xu, X., Wang, L., Bai, G., and Xiang, W. (2015). Low Expression of Mfn2 Is Associated with Mitochondrial Damage and Apoptosis of Ovarian Tissues in the Premature Ovarian Failure Model. PLoS One *10*, e0136421. https://doi.org/10.1371/journal.pone.0136421.
32. Liang, J., Gao, Y., Feng, Z., Zhang, B., Na, Z., and Li, D. (2023). Reactive oxygen species and ovarian diseases: Antioxidant strategies. Redox Biol. *62*, 102659. https://doi.org/10.1016/j.redox.2023.102659.
33. M, R.-D., and Da, A.-B. (2016). Activation of apoptosis signalling pathways by reactive oxygen species. Biochim. Biophys. Acta *1863*, 2977–2992. https://doi.org/10.1016/j.bbamcr.2016.09.012.
34. Yang, D., Wu, X., Wang, W., Zhou, Y., and Wang, Z. (2022). Ciliary Type III Adenylyl Cyclase in the VMH Is Crucial for High-Fat Diet-Induced Obesity Mediated by Autophagy. Adv. Sci. *9*, e2102568. https://doi.org/10.1002/advs.202102568.
35. Zhang, Y., Bai, J., Cui, Z., Li, Y., Gao, Q., Miao, Y., and Xiong, B. (2023). Polyamine metabolite spermidine rejuvenates oocyte quality by enhancing mitophagy during female reproductive aging. Nat. Aging *3*, 1372–1386. https://doi.org/10.1038/s43587-023-00498-8.
36. Wu, X., Yang, D., Zhou, Y., Li, S., and Wang, Z. (2022). The role of ciliopathy-associated type 3 adenylyl cyclase in infanticidal behavior in virgin adult male mice. iScience *25*, 104534. https://doi.org/10.1016/j.isci.2022.104534.
37. Liu, X., Zhou, Y., Yang, D., Li, S., Liu, X., and Wang, Z. (2020). Type 3 adenylyl cyclase in the MOE is involved in learning and memory in mice. Behav. Brain Res. *383*, 112533. https://doi.org/10.1016/j.bbr.2020.112533.
38. Liu, X., Zhou, Y., Li, S., Yang, D., Jiao, M., Liu, X., and Wang, Z. (2020). Type 3 adenylyl cyclase in the main olfactory epithelium participates in depression-like and anxiety-like behaviours. J. Affect. Disord. *268*, 28–38. https://doi.org/10.1016/j.jad.2020.02.041.
39. Wang, Y., Teng, Z., Li, G., Mu, X., Wang, Z., Feng, L., Niu, W., Huang, K., Xiang, X., Wang, C., et al. (2015). Cyclic AMP in oocytes controls meiotic prophase I and primordial folliculogenesis in the perinatal mouse ovary. Development *142*, 343–351. https://doi.org/10.1242/dev.112755.
40. Spinelli, J.B., and Haigis, M.C. (2018). The multifaceted contributions of mitochondria to cellular metabolism. Nat. Cell Biol. *20*, 745–754. https://doi.org/10.1038/s41556-018-0124-1.
41. Victorelli, S., Salmonowicz, H., Chapman, J., Martini, H., Vizioli, M.G., Riley, J.S., Cloix, C., Hall-Younger, E., Machado Espindola-Netto, J., Jurk, D., et al. (2023). Apoptotic stress causes mtDNA release during senescence and drives the SASP. Nature *622*, 627–636. https://doi.org/10.1038/s41586-023-06621-4.
42. Chiaratti, M.R., Garcia, B.M., Carvalho, K.F., Macabelli, C.H., Ribeiro, F.K.d.S., Zangirolamo, A.F., Sarapião, F.D., Seneda, M.M., Meirelles, F.V., Guimarães, F.E.G., and Machado, T.S. (2018). Oocyte mitochondria: role on fertility and disease transmission. Anim. Reprod. *15*, 231–238. https://doi.org/10.21451/1984-3143-AR2018-0069.
43. Zhang, D., Keilty, D., Zhang, Z.F., and Chian, R.C. (2017). Mitochondria in oocyte aging: current understanding. Facts Views Vis. Obgyn *9*, 29–38.
44. van der Reest, J., Nardini Cecchino, G., Haigis, M.C., and Kordowitzki, P. (2021). Mitochondria: Their relevance during oocyte ageing. Ageing Res. Rev. *70*, 101378. https://doi.org/10.1016/j.arr.2021.101378.
45. Zhang, M., Bener, M.B., Jiang, Z., Wang, T., Esencan, E., Scott III, R., Horvath, T., and Seli, E. (2019). Mitofusin 1 is required for female fertility and to maintain ovarian follicular reserve. Cell Death Dis. *10*, 560. https://doi.org/10.1038/s41419-019-1799-3.
46. Ben-Meir, A., Burstein, E., Borrego-Alvarez, A., Chong, J., Wong, E., Yavorska, T., Naranian, T., Chi, M., Wang, Y., Bentov, Y., et al. (2015). Coenzyme Q10 restores oocyte mitochondrial function and fertility during reproductive aging. Aging Cell *14*, 887–895. https://doi.org/10.1111/acel.12368.
47. Wesevich, V., Kellen, A.N., and Pal, L. (2020). Recent advances in understanding primary ovarian insufficiency. F1000Res. *9*. F1000 Faculty Rev-1101. https://doi.org/10.12688/f1000research.26423.1.
48. Mikhael, S., Punjala-Patel, A., and Gavrilova-Jordan, L. (2019). Hypothalamic-Pituitary-Ovarian Axis Disorders Impacting Female Fertility. Biomedicines *7*, 5. https://doi.org/10.3390/biomedicines7010005.
49. McIlwraith, E.K., and Belsham, D.D. (2020). Hypothalamic reproductive neurons communicate through signal transduction to control reproduction. Mol. Cell. Endocrinol. *518*, 110971. https://doi.org/10.1016/j.mce.2020.110971.
50. Chiang, J.L., Shukla, P., Pagidas, K., Ahmed, N.S., Karri, S., Gunn, D.D., Hurd, W.W., and Singh, K.K. (2020). Mitochondria in Ovarian Aging and Reproductive Longevity. Ageing Res. Rev. *63*, 101168. https://doi.org/10.1016/j.arr.2020.101168.
51. Matsuda, F., Inoue, N., Manabe, N., and Ohkura, S. (2012). Follicular growth and atresia in mammalian ovaries: regulation by survival and death of granulosa cells. J. Reprod. Dev. *58*, 44–50. https://doi.org/10.1262/jrd.2011-012.

52. Vaccari, S., Horner, K., Mehlmann, L.M., and Conti, M. (2008). Generation of mouse oocytes defective in cAMP synthesis and degradation: endogenous cyclic AMP is essential for meiotic arrest. Dev. Biol. *316*, 124–134. https://doi.org/10.1016/j.ydbio.2008.01.018.

53. Kong, D., Cho, H., Hwang, S., Choi, E., Lee, A.Y., Choi, E.-K., Kim, Y.-B., Kim, H.-J., and Hong, S. (2023). Bioinformatics and integrated pharmacology network to identify the therapeutic targets and potential molecular mechanism of alpha-lipoic acid on primary ovarian insufficiency. J. Cell. Biochem. *124*, 1557–1572. https://doi.org/10.1002/jcb.30464.

54. Li, H.J., Sutton-McDowall, M.L., Wang, X., Sugimura, S., Thompson, J.G., and Gilchrist, R.B. (2016). Extending prematuration with cAMP modulators enhances the cumulus contribution to oocyte antioxidant defence and oocyte quality via gap junctions. Hum. Reprod. *31*, 810–821. https://doi.org/10.1093/humrep/dew020.

55. Liu, B., Liu, Y., Li, S., Chen, P., Zhang, J., and Feng, L. (2023). BDNF promotes mouse follicular development and reverses ovarian aging by promoting cell proliferation. J. Ovarian Res. *16*, 83. https://doi.org/10.1186/s13048-023-01163-9.

56. Qin, X., Zhao, Y., Zhang, T., Yin, C., Qiao, J., Guo, W., and Lu, B. (2022). TrkB agonist antibody ameliorates fertility deficits in aged and cyclophosphamide-induced premature ovarian failure model mice. Nat. Commun. *13*, 914. https://doi.org/10.1038/s41467-022-28611-2.

57. Wang, X., Wang, L., and Xiang, W. (2023). Mechanisms of ovarian aging in women: a review. J. Ovarian Res. *16*, 67. https://doi.org/10.1186/s13048-023-01151-z.

58. Wickham, H. (2009). ggplot2: Elegant Graphics for Data Analysis (Springer). https://doi.org/10.1007/978-0-387-98141-3.

59. Wu, T., Hu, E., Xu, S., Chen, M., Guo, P., Dai, Z., Feng, T., Zhou, L., Tang, W., Zhan, L., et al. (2021). clusterProfiler 4.0: A universal enrichment tool for interpreting omics data. Innovation *2*, 100141. https://doi.org/10.1016/j.xinn.2021.100141.

STAR★METHODS

KEY RESOURCES TABLE

REAGENT or RESOURCE	SOURCE	IDENTIFIER
Antibodies		
Rabbit Anti-Adenylate Cyclase 3, use 1:1,000 for IF	Novus	Cat#NBP1-92683; RRID: AB_11031204
Rabbit Anti-Caspase3, use 1:200 for IF	Abcam	Cat#ab13847; RRID: AB_443014
Rabbit Anti-Ki67, use 1:500 for IF	Abcam	Cat#ab15580; RRID: AB_443209
Rabbit Anti-DDX4, use 1:1,000 for IF	Thermo Fisher Scientific	Cat#PA5-79147; RRID: AB_2746263
Rabbit Anti-Caspase3, use 1:400 for WB	Abcam	Cat#ab13847; RRID: AB_443014
Rabbit Anti-Adenylate Cyclase 3, use 1:500 for WB	Thermo Fisher Scientific	Cat#PA5-35382; RRID: AB_2552692
Rabbit Anti-DDX4, use 1:500 for WB	Thermo Fisher Scientific	Cat#PA5-79147; RRID: AB_2746263
Mouse Anti-Progesterone Receptor (Alpha PR6), use 1:1,000 for WB	Thermo Fisher Scientific	Cat#MA1-411; RRID: AB_2283820
Rabbit Anti-Bcl-2, use 1:300 for WB	WanLeiBio	Cat#WL01556; RRID: AB_2904235
Rabbit Anti-Bax, use 1:300 for WB	WanLeiBio	Cat#WL01637; RRID: AB_2904236
Rabbit Anti-Inhibin alpha, use 1:400 for WB	WanLeiBio	Cat#WL04690; RRID: AB_3099655
Mouse Anti-Human ER alpha (D-12), use 1:300 for WB	Santa Cruz Biotechnology	Cat#sc-8005; RRID: AB_627556
Rabbit Anti-beta Actin, use 1:2,000 for WB	Proteintech	Cat#20536-1-AP; RRID: AB_10700003
Mouse Anti-GAPDH, use 1:2,000 for WB	Proteintech	Cat#60004-1-Ig; RRID: AB_2107436
Donkey Anti-Rabbit IgG (H+L) Highly Cross-Adsorbed Secondary Antibody, Alexa Fluor™ 488, use 1:1,000	Thermo Fisher Scientific	Cat#A-21206; RRID: AB_2535792
Goat Anti-Rabbit IgG (H+L) Highly Cross-Adsorbed Secondary Antibody, Alexa Fluor™ 594, use 1:1,000	Thermo Fisher Scientific	Cat#A-11037; RRID: AB_2534095
Anti-Mouse IgG (H+L) Antibody, RbSA, Human Serum Adsorbed, DyLight™ 800-Labeled, use 1:10,000	SeraCare KPL	Cat#5230-0416; RRID: AB_2920643
Anti-Rabbit IgG (H+L) Antibody, DyLight™ 800-Labeled, use 1:10,000	SeraCare KPL	Cat#5230-0412; RRID: AB_2753123
Deposited data		
Raw proteomic data	This paper	PRIDE: PXD053066
Oligonucleotides		
INHA-qPCR-F	Sangon Biotech	CCTTTTGCTGTTGACCCTACG
INHA-qPCR-R	Sangon Biotech	AGGCATCTAGGAATAGAGCCTTC
AMH-qPCR-F	Sangon Biotech	CCACACCTCTCTCCACTGGTA
AMH-qPCR-R	Sangon Biotech	GGCACAAAGGTTCAGGGGG
hADCY3-qPCR-F	Sangon Biotech	CGCACAGTTCTAGCTGATCAGT
hADCY3-qPCR-R	Sangon Biotech	CTGAGGGCCTCTTCTTTGTCTG
GAPDH-qPCR-F	Sangon Biotech	GGTGAAGGTCGGTGTGAACG
GAPDH-qPCR-R	Sangon Biotech	CTCGCTCCTGGAAGATGGTG
Adcy1-RT-PCR-F	Sangon Biotech	GTCACCTTCGTGTCCTATGCC

(*Continued on next page*)

Continued

REAGENT or RESOURCE	SOURCE	IDENTIFIER
Adcy1-RT-PCR-R	Sangon Biotech	TTCACACCAAAGAAGAGCAGG
Adcy2-RT-PCR-F	Sangon Biotech	GACTGGCTCTACGAGTCCTAC
Adcy2-RT-PCR-R	Sangon Biotech	GGGCAGTGGGAACGGTTAT
Adcy3-RT-PCR-F	Sangon Biotech	CTCGCTTTATGCGGCTGAC
Adcy3-RT-PCR-R	Sangon Biotech	ACATCACTACCACGTAGCAGT
Adcy4-RT-PCR-F	Sangon Biotech	AGTACCCACTGCTGATACTGC
Adcy4-RT-PCR-R	Sangon Biotech	AGCCACCCAAAGCACACAG
Adcy5-RT-PCR-F	Sangon Biotech	GGCGGCAACCAGGTGTCAAAGG
Adcy5-RT-PCR-R	Sangon Biotech	CCCAGAAACTCGTCCACTTCATCCT
Adcy6-RT-PCR-F	Sangon Biotech	TGAGTCTTCTAGCCAGCTCTG
Adcy6-RT-PCR-R	Sangon Biotech	CAGCACCAAGTAGGTGAACCC
Adcy7-RT-PCR-F	Sangon Biotech	AAGGGGCGCTACTTCCTAAAT
Adcy7-RT-PCR-R	Sangon Biotech	GTGTCTGCGGAGATCCTCA
Adcy8-RT-PCR-F	Sangon Biotech	CTCTACACCATCCAACCGACG
Adcy8-RT-PCR-R	Sangon Biotech	GCACCGAGTCGCTAGACAG
Adcy9-RT-PCR-F	Sangon Biotech	CAACAGCGTGAGGGTCAAGAT
Adcy9-RT-PCR-R	Sangon Biotech	CATGGAGTCGAATTTGGGGTC
Adcy10-RT-PCR-F	Sangon Biotech	GGCAGGAATTACAAGACAGGG
Adcy10-RT-PCR-R	Sangon Biotech	GCACTTTCTCCACTATGGCACT
Software and algorithms		
ImageJ	NIH	https://imagej.nih.gov/ij/
Proteome Discoverer™ software	Thermo Fisher Scientific, version 2.2	https://knowledge1.thermofisher.com/Software_and_Downloads/Chromatography_and_Mass_Spectrometry_Software/Proteome_Discoverer/Proteome_Discoverer_Operator_Manuals/Proteome_Discoverer_2.2_overview
GraphPad Prism	GraphPad Software Inc	http://www.graphpad.com/
ggplot2 packages	Wickham et al.[58]	https://ggplot2.tidyverse.org.
R packages	Wu et al.[59]	https://www.bioconductor.org/packages/release/bioc/html/clusterProfiler.html

RESOURCE AVAILABILITY

Lead contact

Further information and requests for resources and reagents should be directed to and will be fulfilled by the lead contact, Zhenshan Wang (zswang@hbu.edu.cn).

Materials availability

This study did not generate new unique reagents.

Data and code availability

- Raw proteomic data have been deposited to the ProteomeXchange Consortium via the PRIDE and are publicly available as of the date of publication. Accession numbers are listed in the key resources table.
- This paper does not report original code.
- Any additional information required to reanalyze the data reported in this paper is available from the lead contact upon request.

EXPERIMENTAL MODEL AND STUDY PARTICIPANT DETAILS

Animals

The Adcy3 KO mice (C57BL/6) were obtained from the Storm laboratory of the University of Washington, Seattle. To obtain the control and Adcy3 KO female mice, reproduction and offspring genotyping was performed on Adcy3$^{+/-}$ mice. hADCY3 knock-in mice were generated in the lab. Female mice aged at 2 days, 7 days, 30 days, 60 days, 90 days, 120 days, and 10-12 months were used in this study. The DNA obtained from the tail is used for genotyping using the following primers:

Adcy3 control (Adcy300): 5′-CTGGTGAAGTGGCTTGACCT-3′,
Adcy3 control (Adcy910): 5′-GTTATGAAGAAGGAGAAGACA-3′,
Adcy3 KO: 5′-CTGTGAAGTAGGTTCCTACCTG-3′,
Adcy3 KO: 5′-CCTGTGCTCTAGTAGCTTTACGG-3′.

All experimental mice were housed in a pathogen free-environment (SPF) with temperature control (23 ± 1°C) and humidity control (60 ± 10%), and randomly obtained water and conventional rodent food during a 12-hour light/12-hour dark cycle. Animal handling and use followed a protocol approved by the Animal Care and Use Committee of Hebei University (approval no.: IACUC-2023005XR).

METHOD DETAILS

Fertility assay

Control and Adcy3 KO female mice at PD60 were housed together with WT C57BL/6N males (2-3 months old), which have been shown to be fertile. Mating plugs were monitored daily, and females with significantly enlarged abdomens were moved to separate cages to monitor pregnancy. The mating process lasted for 6 months. The number of pups was counted on the first day after birth.

Gonadosomatic index and histological analysis

Control and Adcy3 KO female mice at PD30 and PD60 were weighed, and the ovaries were dissected and weighed. The relative gonadosomatic index of the ovaries/body weight was calculated using the following equation: Gonadosomatic index = (ovary weight/body weight) × 100%. Ovaries were collected and fixed in 4% polyformaldehyde (PFA) overnight, dehydrated through a series of graded ethanol solutions and xylene, and embedded in paraffin. The thickness of the ovarian sections was 6 μm. The samples were stained with hematoxylin and eosin (H&E), and images were taken using an Olympus fluorescence microscope. The total number of follicles at all stages was counted and quantified.

Estrus cycle determination

The estrus cycle was examined by H&E staining of mouse vaginal smears taken daily for a period of 21 days. Saline solution was injected into the mouse vagina. The cells were collected on glass slides, and the slides were air-dried, fixed, stained, and examined under an optical microscope to determine the estrus cycle presence and stage.

Serum hormone measurements

Before estrus (by observing appearance), PD90 control and KO mice were euthanized to avoid ovulation. Blood was collected retro-orbitally, and the serum was separated and stored at -80°C until use. The serum levels of FSH, LH, estrogen, and testosterone were measured via ELISA.

Superovulation and oocyte collection

At PD30, female mice were injected with pregnant mare's serum gonadotropin (PMSG, 10 IU) before being euthanized. The ovaries were dissected and completely punctured in M2 medium (Solarbio, China), the oocyte-cumulus complexes were collected, and the oocytes with an intact zona pellucida were collected as GV-phase oocytes. The oocytes were further cultivated in M16 medium (Sigma, USA) supplemented with mineral oil. At PD90, female mice were injected with PMSG (10 IU), followed by human chorionic gonadotropin (hCG, 10 IU) 48 h later. The female mice were euthanized, and cumulus-oocyte complexes and MII oocytes were collected from the oviducts 14 h after hCG injection.

RNA isolation, qPCR quantification and RT-PCR

Total RNA was isolated from PD30 ovaries or isolated oocytes using the RNeasy Micro Kit (217084, QIAGEN), and first-strand cDNA was synthesized using a PrimeScipt™ RT reagent Kit with gDNA eraser (R323-01, Vazyme). The qPCR was performed with Nova™ SYBR Green PCR Master Green mix (R712, Vazyme). Gene expressions were normalized to *GAPDH* levels and were determined by the $2^{-\Delta\Delta CT}$ method. Primers used are listed in key resources table.

Western blot

Oocytes and ovaries were lysed in lysis buffer (P0013, Beyotime) with a protease inhibitor cocktail (100 ×) (5871, Cell Singling Technology) on ice. Protein concentrations were measured by BCA assay (Solarbio, China). Proteins were separated by SDS–PAGE and transferred to a PVDF membrane (RINB77899, Millipore). The membrane was blocked for 1 h in TBS plus 5% nonfat milk, followed by incubation at 4°C overnight or

at room temperature (RT) for 2–3 h with primary antibodies. After three washes with TBST, the membrane was incubated with secondary antibodies at RT for 1 to 2 h. Images were obtained using Odyssey software (Gene). Antibodies used in this study are listed in key resources table.

Immunofluorescence and image analysis

The isolated ovaries were fixed with 4% PFA for 24 h, then embedded in paraffin and sliced. After the paraffin section is dewaxed and rehydrated, the samples were permeabilized by 0.5% Triton X-100 for 15 min. After blocking in 5% goat serum at RT for 3 h, the ovarian sections were incubated with primary antibodies overnight at 4°C. The next day, the ovarian sections were washed with PBS, and incubated with the secondary antibodies for 2 h, and then mounted with anti-fluorescence quenching sealing agent containing DAPI and dry it in dark. Images were taken using an Olympus confocal microscope (FV3000, Olympus, Japan). Antibodies used in this study are listed in key resources table.

TUNEL assay and EdU labeling

Ovaries were fixed in 4% PFA, dehydrated, embedded in paraffin, sectioned to 6 μm, and were analyzed using the terminal deoxynucleotide transferase nick end labeling (TUNEL) assay (Promega, G3250) to evaluate the numbers of apoptotic cells between control and Adcy3 KO ovaries.

Female mice at PD30 were intraperitoneally injected with 50 mg/kg EdU. After 2 h of injection, the mice were euthanized through cervical dislocation, the ovaries were separated and fixed in 4% PFA for 24 h, and then embedded in OCT compound. The ovarian sections were incubated with Cell Light EdU Apollo 488 *in vitro* kit according to the manufacturer's instructions (Ribobio, C10310-3). The images were taken using an Olympus FLUOVIEW FV3000 microscope.

Proteome analysis

Ovaries were collected from control and Adcy3 KO female mice and were quickly transferred in liquid nitrogen. Frozen ovaries were lysed with lysis buffer supplemented with protease inhibitors. A total of 100 μg protein was resuspended in 5 mM dithiothreitol for 45 min at 37°C, followed by alkylation with 20 mM iodoacetamide at RT for 30 min and digestion with trypsin (Promega) for 16 h at 37°C. The digested peptides were desalted using a Sep-Pak C18 column (Agilent Technologies, A57003100). The peptides were then lyophilized, reconstituted in 0.1% formic acid, and analyzed using a Q Exactive Mass Spectrometer (Thermo Fisher Scientific) coupled to an UltiMate 3000 RSLC Systems (Thermo Fisher Scientific). The spectral data were analyzed using the Proteome Discoverer™ software (Thermo Fisher Scientific, version 2.2) by searching against the mouse proteins in the UniProt database. Subsequent identification of the results was performed using the bitr function from the clusterProfiler package in R. The results were further filtered and refined using the dplyr package in R. For Gene Ontology (GO) and Kyoto Encyclopedia of Genes and Genomes (KEGG) enrichment analyses, the enrichGO and enrichKEGG functions from the clusterProfiler package were utilized. Visualization of all these results were conducted using the ggplot2 package in R.[58,59]

β-Galactosidase staining

According to β-SA-Instructions of the galactosidase test kit (Beyotime, China), frozen ovarian sections β-Galactosidase staining was used to evaluate the aging of follicular cells in the ovaries of PD90 female mice.

Mitochondrial distribution in oocytes

The mitochondrial distribution was examined by staining with MitoTracker Red (Beyotime, China) using the oocytes at MII from control and Adcy3 KO females. After washing three times with M2 medium, the oocytes were imaged using Olympus FLUOVIEW FV3000 confocal microscope.

ROS level determination in oocytes

Oocytes from different groups were treated as indicated and incubated with M2 medium containing 10 μM DCFH-DA (Beyotime, China) at 37°C for 20 min. After washing three times with M2 medium, the oocytes were imaged using Olympus FLUOVIEW FV3000 confocal microscope. The mean fluorescent intensity of oocytes was quantified using Image J software.

QUANTIFICATION AND STATISTICAL ANALYSIS

Statistical analyses were performed in GraphPad Prism 9.0 using Student's two-tailed t-test or ANOVA. All data were presented as mean ± SD. Differences were considered significant if $p < 0.05$ (*$p < 0.05$, **$p < 0.01$, ***$p < 0.001$, **** $p < 0.0001$).